Recognition Characteristics of Monoclonal Antibodies That Are Cross-Reactive with Gangliosides and Lipooligosaccharide from *Campylobacter jejuni* Strains Associated with Guillain-Barré and Fisher Syndromes†

R. Scott Houliston,‡ Nobuhiro Yuki,§ Tomoko Hirama,‡ Nam H. Khieu,‡ Jean-Robert Brisson,‡ Michel Gilbert,*,‡ and Harold C. Jarrell*,‡

Institute for Biological Sciences, National Research Council Canada, Ottawa, Ontario K1A 0R6, Canada, and Department of Neurology and Research Institute for Neuroimmunological Diseases, Dokkyo Medical University School of Medicine, Tochigi, Japan

Received September 26, 2006; Revised Manuscript Received November 2, 2006

ABSTRACT: The enteropathogen *Campylobacter jejuni* has the ability to synthesize glycan structures that are similar to mammalian gangliosides within the core component of its lipooligosaccharide (LOS). Exposure to ganglioside mimics in some individuals results in the production of autoantibodies that deleteriously attack nerve surface gangliosides, precipitating the onset of Guillain-Barré and Fisher syndromes (GBS and FS). We have characterized the interaction of four monoclonal antibodies (mAbs), established by sensitization of mice with LOS isolated from GBS- and FS-associated *C. jejuni* strains, with chemoenzymatically synthesized gangliooligosaccharides. Surface plasmon resonance (SPR) measurements demonstrate that three of the mAbs interact specifically with derivatives corresponding to their targeted gangliosides, with dissociation constants ranging from 10 to 20 μM. Antibody binding to the gangliooligosaccharides was probed by saturation transfer difference (STD) NMR spectroscopy. STD signals, resulting from antibody/oligosaccharide interaction, were observed for each of the four mAbs. In two cases, differential saturation transfer rates to oligosaccharide resonances enabled detailed epitope mapping. The binding of GD1a-S-Phe with GB1 is characterized by close association of the immunoglobulin with sites that are distributed over several residues of the oligosaccharide. This contrasts sharply with the profile observed for the binding of both GD3-S-Phe and GT1a-S-Phe with FS1. The close antigenic contacts in these ganglioside derivatives are confined to the *N*-acetylmannosaminyl portion of the terminal *N*-acetylneuraminic acid (NeuAc) residue of the disialosyl moiety. Our characterization of FS1 provides insight, at an atomic level, into how a single antigenic determinant presented by the LOS of *C. jejuni* can give rise to antibodies with binding promiscuity to [αNeuAc-(2−8)-αNeuAc]-bound epitopes and demonstrates why sera from FS patients have antibodies that are often reactive with more than one disialylated ganglioside.

As a mechanism to evade immune response, pathogenic microorganisms often display surface glycans that closely resemble those of their host. This form of molecular mimicry has been postulated to trigger the production of antibodies that cross-react with epitopes common to both the pathogen and host, leading to an autoimmune disease (*1*−*3*). Guillain-Barré and Fisher syndromes (GBS and FS)[1] are immune-mediated neuropathies that arise as a result of the presence of autoantibodies targeted against gangliosides, which are found in abundance in nerve tissue. GBS is characterized by the acute onset of limb weakness and areflexia. In FS, which is a variant of GBS, neurological damage is confined mainly to the eye muscles. Because the majority of individuals with GBS and FS show signs of an infection 1−3 weeks prior to the development of symptoms, these two conditions have emerged as prototypes used to elucidate the complex mechanisms governing the onset of a postinfectious autoimmune response triggered by molecular mimicry (*1*−*3*).

There is a substantial body of data to demonstrate that pathogen-bound ganglioside mimics are causative agents prompting autoantibody production in individuals with GBS and FS (*3*). Studies focused on the involvement of the enteropathogen *Campylobacter jejuni* have provided some of the strongest evidence in support of this assertion. This bacterium is the most frequently identified infectious agent that precedes the onset of GBS and FS (*4*, *5*). The glycan component of its lipooligosaccharide (LOS) is often sialylated and structurally similar to mammalian gangliosides (*5*−*9*). Antiganglioside IgGs and IgMs have been raised in mice inoculated with LOS from *C. jejuni*, and these antibodies

†This study was supported by a grant from the Human Frontier Science Program (RGP 38/2003).

* To whom correspondence should be addressed. M.G.: tel, (613) 991-9956; fax, (613) 952-9092; e-mail, Michel.Gilbert@nrc-cnrc.gc.ca. H.C.J.: tel, (613) 993-5900; fax, (613) 952-9092; e-mail, Harold.Jarrell@nrc-cnrc.gc.ca.

‡ National Research Council Canada.

§ Dokkyo Medical University School of Medicine.

[1] Abbreviations: GBS, Guillain-Barré syndrome; FS, Fisher syndrome; LOS, lipooligosaccharide; mAb, monoclonal antibody; NeuAc, *N*-acetylneuraminic acid; SPR, surface plasmon resonance; STD, saturation transfer difference.

10.1021/bi062001v CCC: $37.00
Published on Web 01/02/2007

can mediate the blocking of nerve cell action potentials in vitro (*10*). Furthermore, immunization of rabbits with GM1a-like LOS can induce the production of anti-GM1a IgG antibodies leading to flaccid paralysis (*11*, *12*).

Epidemiological studies have confirmed that the vast majority of GBS- and FS-associated *C. jejuni* strains carry genes required for the synthesis of sialylated LOS (*7*, *13*, *14*). More specifically, strains which express GM1a-like and GD1a-like LOS are most commonly isolated from GBS patients, whereas those associated with FS commonly synthesize GT1a-like and GD1c-like LOS, which are similar to GQ1b (*7*, *13*). This is consistent with the observation that the motor neurons of limb muscles affected in patients with GBS express GM1a and GD1a, while GQ1b is expressed in the oculomotor nerves and primary sensory neurons that are implicated in FS (*15*).

While the nature and prevalence of molecular mimics presented by infectious agents causing GBS and FS have been extensively examined, and the pathophysiological consequences resulting from autoantibody production in individuals suffering from these conditions have been elucidated, critical details underlying how and why destructive autoantibodies are produced in selected individuals following exposure to a molecular mimic remain unknown. Investigations focused on the binding characteristics of the key mediators of these conditions, the cross-reactive antibodies, have been limited almost exclusively to immunostaining techniques or immunoadsorption assays such as ELISA. While used successfully to elucidate the common structures recognized by the antibodies, these studies have provided limited scope for the understanding of antigen recognition at a molecular level.

In this report, we describe the binding characteristics of monoclonal antibodies (mAbs), raised in mice against LOS isolated from GBS- and FS-associated *C. jejuni* strains, using chemoenzymatically synthesized gangliooligosaccharides. We provide, for the first time, measurements of the kinetics for gangliooligosaccharide binding to cross-reactive mAbs, obtained through surface plasmon resonance (SPR). For two antibodies, we have mapped their ligand recognition site at atomic resolution using saturation transfer difference (STD) NMR spectroscopy.

MATERIALS AND METHODS

Monoclonal Antibodies. Clones GB1 and GB2 were obtained from a mouse inoculated with LOS from *C. jejuni* strain CF90-26, which was isolated from a patient with GBS (*5*, *12*). An ELISA showed that GB1 (IgG3κ) reacted strongly with GD1a and weakly with GT1b and that GB2 (IgG2bκ) reacted strongly with GM1a and weakly with GT1b. Thin-layer chromatography with immunostaining showed that both GB1 and GB2 react with CF90-26 LOS. Clones FS1 and FS3 were obtained from mice inoculated with either the LOS or heat-killed cell lysate, respectively, of *C. jejuni* strain CF93-6. This strain was isolated from a patient with FS (*5*). On the basis of ELISA measurements, FS1 (IgG3κ) reacted with GD3 as well as GT1a and GQ1b, whereas FS3 reacted with GT1a and GQ1b. Both FS1 and FS3 were shown to bind to CF93-6 LOS by immunostaining. The four hybridoma clones were cultured in DMEM medium containing 10% FBS (Ultra-Low IgG grade; GIBCO). The mAbs were purified with HiTrap protein A HP columns (Amersham Pharmacia) according to the manufacturer's instructions.

Gangliooligosaccharide Synthesis. Multimilligram quantities of thiophenyl derivatives corresponding to the glycan component of GM3, GD3, GM2, GM1a, GD1a, and GT1a were synthesized chemoenzymatically for use in this study. The *C. jejuni* glycosyltransferases CgtA, CgtB, Cst-I, and Cst-II, which have β-(1→4)-*N*-acetylgalactosaminyltransferase, β-(1→3)-galactosyltransferase, α-(2→3)-sialyltransferase, and α-(2→3/8)-sialyltransferase activity, respectively, were expressed in *Escherichia coli* and purified as described previously (*16*−*18*). Starting initially with β-D-Gal*p*-(1,4)-β-D-Glc*p*-S-Phe, kindly provided by Dr. Dennis Whitfield, GM3- and GD3-S-Phe were synthesized sequentially using the enzymes Cst-I and Cst-II, respectively. GM2- and GM1a-S-Phe were synthesized from GM3-S-Phe using CgtA and CgtB, respectively. Finally, GD1a- and GT1a-S-Phe were synthesized sequentially from GM1a-S-Phe using the enzymes Cst-I and Cst-II, respectively. The progress of each enzymatic addition was monitored by TLC, and the desired products were separated from contaminating reactants by passing the material through Sep-Pak columns (Waters Corp.). Final purification of GD3-, GD1a-, and GT1a-S-Phe was achieved by anion-exchange chromatography using a MiniQ column on an AKTA explorer system (Amersham Biosciences). NaCl was removed from the purified glycan derivatives using HiTrap desalting columns (Amersham Biosciences). Purification of GM3-, GM2-, and GM1a-S-Phe by ion-exchange chromatography was not necessary, as these compounds were found to be at >90% purity following Sep-Pak treatment. All of the thiophenyl derivatives were quantified by obtaining UV adsorption readings in H_2O at 245 nm ($\epsilon = 5.9$ cm^{-1} mM^{-1}).

Gangliooligosaccharide Characterization by NMR Spectroscopy. The structures of the GD3-, GM1a- GD1a-, and GT1a-S-Phe derivatives were confirmed by NMR spectroscopy. Spectra of the compounds were acquired in both D_2O and H_2O/D_2O (90%/10%) on Varian spectrometers, operating at 500 and 600 MHz, at 25 °C. Standard ^{1}H−^{1}H COSY, TOCSY, and NOESY spectra and ^{1}H−^{13}C HSQC and HMBC spectra were acquired to assign the ^{1}H and ^{13}C resonances and to confirm the structure of the oligosaccharides. Selective 1D-TOCSY and 1D-TOCSY-TOCSY spectra (*19*) were obtained in order to confirm the ^{1}H assignment of *N*-acetylneuraminic acid (NeuAc) resonances. ^{1}H and ^{13}C shifts were referenced with respect to the methyl group of an internal acetone standard appearing at 2.225 and 31.1 ppm, respectively.

SPR Measurements. The binding kinetics for the interaction of chemoenzymatically synthesized gangliooligosaccharides with the isolated mAbs were determined by SPR using a BIACORE 3000 biosensor system (Biacore, Inc., Piscataway, NJ). Approximately 10000−15000 RUs of IgGs were immobilized on a research grade CM5 sensor chip (BIACORE). This chip was ideally suited for our study, because it enabled the immobilization of large amounts of antibody, which gave rise to a strong SPR response upon injection with the low molecular weight oligosaccharides. No problems were encountered with nonspecific binding, which would have necessitated the use of other sensor chips. Immobilizations were carried out at antibody concentrations of approximately 50 μg/mL in 10 mM acetate buffer (pH

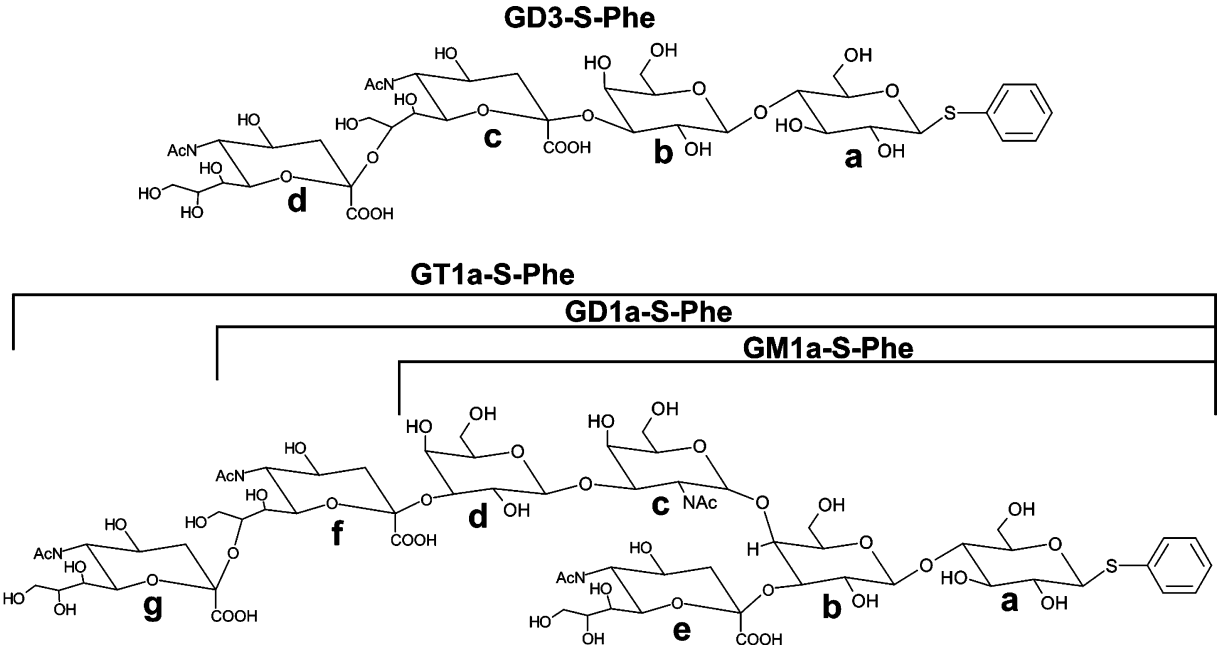

FIGURE 1: Structures of chemoenzymatically synthesized ganglioligosaccharides targeted by mAbs raised against LOS. Clones GB1, GB2, FS1, and FS3 were obtained following the inoculation of mice with LOS from the GBS- and FS-associated *C. jejuni* strains CF90-26 and CF93-6. On the basis of ELISA measurements GB1 binds to the ganglioside GD1a and GB2 with the ganglioside GM1a (*5*). FS1 interacts with both GD3 and GT1a, while FS3 binds to GT1a. Thiophenyl derivatives corresponding to the glycan components of the principal targets of the four mAbs were synthesized chemoenzymatically in multimilligram quantities using *C. jejuni* enzymes involved in LOS biosynthesis.

4.5), using the amine coupling kit supplied by the manufacturer. As a reference protein, *Salmonella* O-chain-specific IgG was immobilized at a similar surface density and under identical conditions. In all instances, analyses were carried out at 25 °C in 10 mM HEPES (pH 7.4), containing 150 mM NaCl, 3 mM EDTA, and 0.005% P20 at a flow rate of 20 μL/min. No regeneration was required. Data were evaluated using the BIAevaluation 4.1 software (Biacore, Inc.).

STD NMR Spectroscopy. Monoclonal antibodies were concentrated using Amicon centrifugal filters (3 kDa cutoff, Millipore) and exchanged several times with a deuterated 50 mM phosphate buffer (pD 7.3), containing 150 mM NaCl. The mAb preparations were combined with freeze-dried ganglioligosaccharide derivates at molar ratios ranging from 1:25 to 1:75; the final oligosaccharide concentrations were between 1 and 2 mM.

STD NMR spectra were acquired at 25 °C on a Varian spectrometer operating at 600 MHz, equipped with a cryogenically cooled probe. Saturation of the antibody resonances was achieved using a train of Gaussian-shaped pulses, with bandwidths of 300 Hz, centered at −1.0 or 9.0 ppm. Similar results were obtained when protein saturation pulses were centered up- or downfield. Phase cycling was used to subtract reference spectra, where saturation pulses were centered at 30 ppm, from those where antibody resonances were excited. For each mAb/oligosaccharide pair investigated, spectra were acquired at several different saturation times, ranging from 50 to 3500 ms. The number of transients varied from 1024 to 4096, depending on the signal intensity of a given sample. The relaxation delay was 2.5 s, and the acquisition time was 1.9 s. A spin-lock filter of 10 ms was used to suppress the protein background. Relative STD values for specific resonances are reported as a percentage of the signal intensity obtained in relation to ^{1}H 1D spectra of the free oligosaccharides. A 2D STD-TOCSY spectrum was acquired to study FS1/GD3-S-Phe association with 400 increments acquired over a sweep width of 6000 Hz in the indirect dimension, using 256 transients per increment and a mixing time of 80 ms. All NMR data were processed using the software TOPSPIN (Bruker Biospin, Billerica, MA).

Molecular Modeling of the Oligosaccharide Component of GD1a. A minimum energy conformation for the oligosaccharide component of GD1a was calculated using an in-house program applying the Metropolis Monte Carlo (MMC) algorithm (*20*). Monosaccharide coordinates were taken from a carbohydrate database with hydrogen atoms deleted and placed at standard geometries. Pyranose rings were kept rigid in the $^4C_1$ conformation or, in the case of NeuAc, the $^2C_5$ conformation. Glycosidic bond angles were also fixed at 117°. The initial glycosidic tortional angles (Φ,Ψ), where $\Phi = O_R{-}C1{-}O1{-}C_X$ and $\Psi = C1{-}O1{-}C_X{-}C_{X-1}$ (with R and X being the glyconic and aglyconic sites, respectively), were chosen from potential energy maps of its disaccharide constituents. The simulation was performed at 2000 K with 100000 macrosteps following a 5000 step equilibration period, employing a MM3 force field. A step length of 10° was used for both sugar linkage and group variations. Transferred NOE (trNOE) experiments were performed at several mixing times for GD1a-S-Phe (data not shown) in the presence of the antibody GB1, in order to acquire distance restraints for the bound conformation of the oligosaccharide, which could be used in the construction of a molecular model. No differences in the internuclear connectivity patterns for the bound and unbound states of the molecule were observed, suggesting similar structures. A conformational study of free GD1a oligosaccharide, based in part on NOE data, has been published previously (*21*).

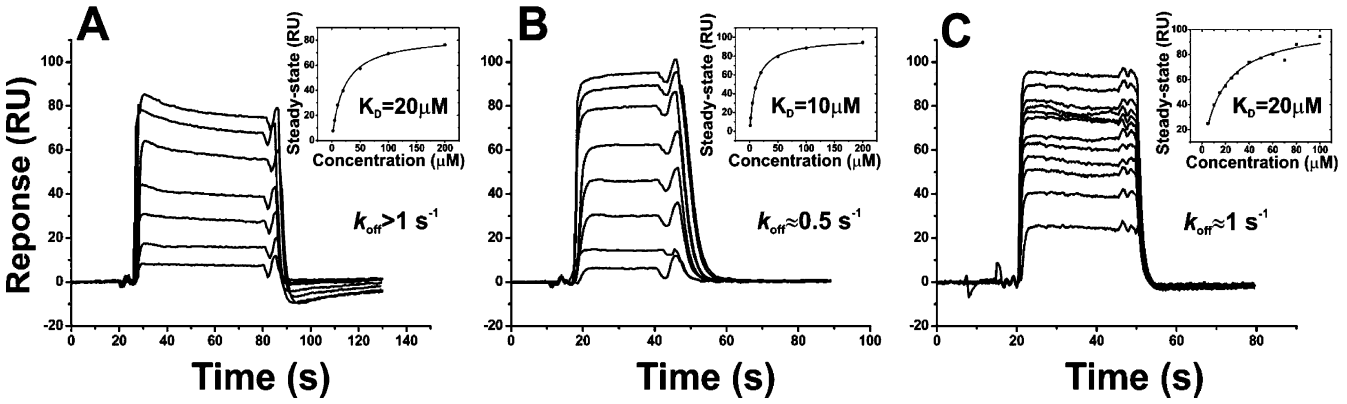

FIGURE 2: Binding kinetics for the interaction of the mAbs with their associated gangliooligosaccharides as determined by SPR. Displayed are sensorgram overlays for the binding of (A) GD1a-S-Phe with GB1, (B) GM1a-S-Phe with GB2, and (C) GT1a-S-Phe with FS3 at oligosaccharide concentrations ranging from 2 to 200 μM. Insets show the steady-state affinity curves used to determine the K_D for each of the antigen/mAb systems. Dissociation rates (k_{off}) were also obtained from the sensorgram data; however, in the case of GD1a-S-Phe/GB1, k_{off} was more rapid than the detection limit for the instrument (>1 s^{-1}). Each mAb was probed with the complete array of oligosaccharides that were synthesized (i.e., GM3-, GD3-, GM2-, GM1a-, GD1a-, and GT1a-S-Phe); however, binding was only observed for these three oligosaccharide/mAb combinations.

RESULTS

Gangliooligosaccharide Synthesis. Starting with β-D-Gal*p*-(1,4)-β-D-Glc*p*-S-Phe, we synthesized multimilligram quantities of oligosaccharides corresponding to the glycan component of gangliosides GD3, GM1a, GD1a, and GT1a (Figure 1), using the enzymes CgtA, CgtB, Cst-I, and Cst-II. These four derivatives correspond to the principal ganglioside targets of the mAbs isolated from mice injected with *C. jejuni* LOS, as determined by ELISA (*5*). Two-dimensional homo- and heteronuclear NMR spectra were acquired to confirm their structure and to assign the chemical shift of ^{1}H and ^{13}C resonances. These assignments are provided as Supporting Information.

Binding Kinetics of Gangliooligosaccharides with Their Corresponding mAbs. SPR was used to confirm whether the mAbs, raised against bacterial LOS, would interact specifically with chemoenzymatically synthesized ganglioside derivatives. Oligosaccharides were injected over immunoglobulins immobilized at high density by amine coupling, on CM5 sensor chips. Binding was assayed individually with GM3-, GD3-, GM2-, GM1a-, GD1a-, and GT1a-S-Phe. For the mAb GB1, a response was observed only upon injection with GD1a-S-Phe, and analysis of the equilibrium data for their interaction yielded a K_D of 20 μM (Figure 2). GB2 was found to interact only with GM1a-S-Phe ($K_D = 10$ μM) and FS3 with only GT1a-S-Phe ($K_D = 10$ μM). The dissociation rates (k_{off}) governing mAb/oligosaccharide binding were also determined to be in the range of 0.5 and 1 s^{-1} for the GM1a-S-Phe/GB2 and GT1a-S-Phe/FS3 pairs, respectively, while the k_{off} for GB1 binding to GD1a-S-Phe was too rapid to be determined (Figure 2). There was effectively no quantifiable interaction of the mAb FS1 with any of the gangliooligosaccharides, including the thiophenyl derivatives of GD3 and GT1a, which were shown to react with this antibody on the basis of ELISA. It is likely that, for FS1, monovalent interaction with its corresponding antigens was too weak to be characterized by this technique.

STD Attenuation of Oligosaccharide Resonances upon Interaction with mAbs. STD NMR has been applied as a method to assay for protein binding to libraries of potential targets (*22*, *23*) and, in investigations with aims similar to ours, as a means of mapping the binding epitope of a ligand at atomic resolution. The recognition characteristics of several carbohydrate- (*22*, *24*−*33*), peptide- (*34*−*36*), and nucleotide-binding proteins (*37*) have been studied using STD NMR. STD signals arise as a result of *through-space* intermolecular magnetization transfer from selectively saturated resonances of a macromolecule to a bound ligand.

When GB1, GB2, and FS3 were incubated in the presence of their targeted oligosaccharides, there were observable STD signals. Plots of relative saturation levels as a function of saturation time for specific oligosaccharide resonances are presented in Figure 3. On the basis of SPR analysis, there was negligible binding of FS1 to any of the chemoenzymatically synthesized gangliooligosaccharides. ELISA measurements showed that this mAb recognizes the disialosyl-containing molecules GT1a and GD3 (*5*). STD spectra acquired for FS1 in the presence of either GD3-S-Phe or GT1a-S-Phe are consistent with saturation transfer from mAb resonances to the oligosaccharide, confirming that this mAb recognizes the glycan component of these two gangliosides (Figure 3C). These STD signals are not a result of nonspecific interaction, as incubation of FS1 with either GD1a-S-Phe or GM1a-S-Phe did not give rise to observable saturation transfer.

For STD NMR to be used effectively to provide an epitope map, ligand protons in close proximity to the macromolecule must experience a higher degree of saturation than those situated at a greater distance. Unfortunately, in some instances, all of the ligand protons will experience a similar STD response, irrespective of their proximity to the macromolecule. This occurs as a result of a relay of saturation from proton to proton within the ligand, also referred to as spin diffusion, and is the result of a slow ligand dissociation rate (k_{off}). For two of the antibody/oligosaccharide combinations, FS3/GT1a and GB2/GM1a, there was uniform saturation of the oligosaccharide proton resonances (Figure 3A). For these two systems, intramolecular spin diffusion appears to have prevented effective epitope mapping. When GB1 and FS1 were incubated with their targeted oligosaccharides, however, there was a differential buildup of magnetization transfer to the ligand protons (Figure 3B,C). In these two

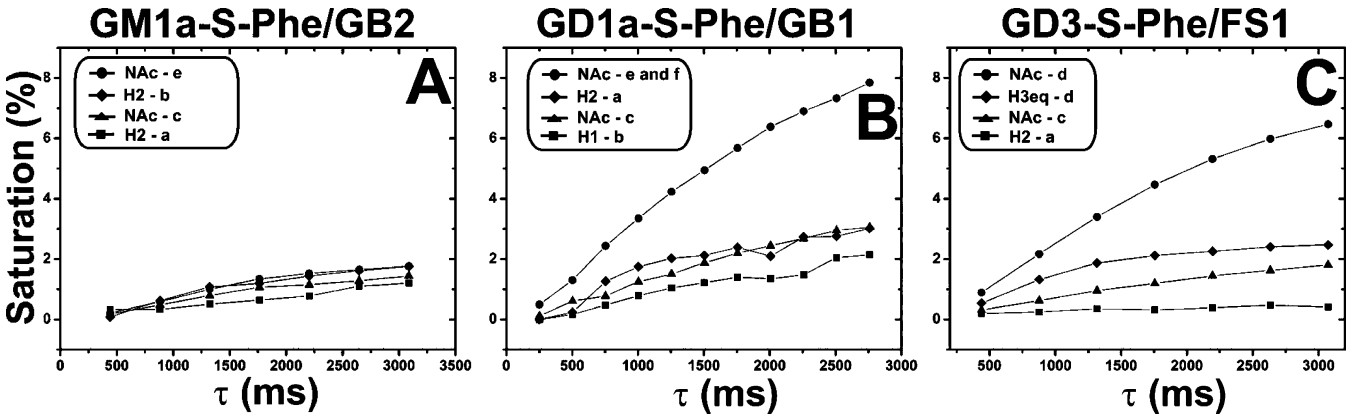

FIGURE 3: STD signals resulting from ganglioooligosaccharide binding to the mAbs. Shown are representative build-up curves resulting from the interaction of (A) GM1a-S-Phe with GB2, (B) GD1a-S-Phe with GB1, and (C) GD3-S-Phe with FS1. GM1a-S-Phe resonances are only weakly enhanced in STD spectra and exhibit a uniform build-up rate. Similar uniform STD build-up curves are obtained for GT1a-S-Phe binding to FS3 (data not shown). In contrast, GD1a-S-Phe and GD3-S-Phe protons exhibit differential build-up rates as a result of binding to GB1 and FS1, respectively, thereby providing insight into ganglioside recognition. The residues are labeled on the basis of the structures presented in Figure 1.

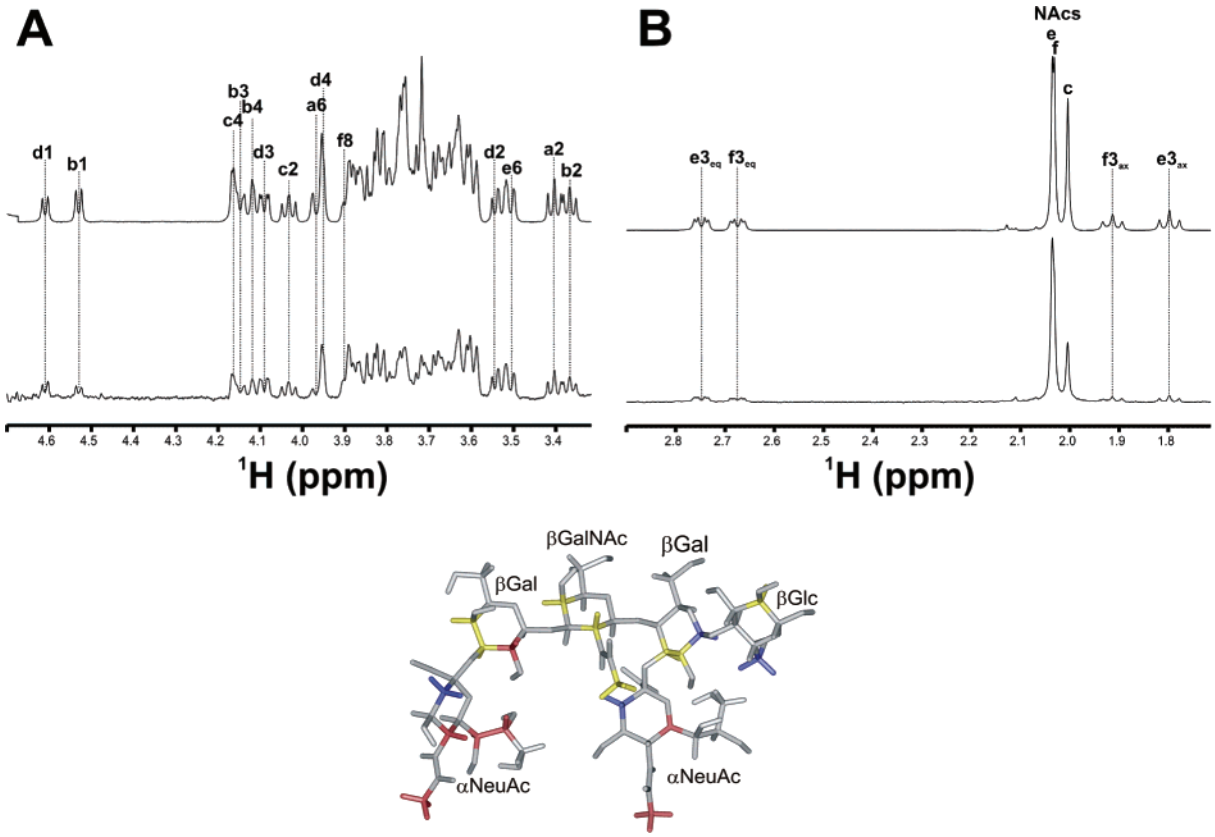

FIGURE 4: Close antigenic contacts between GD1a-S-Phe and GB1 are distributed over several residues of the oligosaccharide. Displayed are the (A) H-ring and (B) *N*-acetyl regions of a 1D ^{1}H spectrum of GD1a-S-Phe (top) overlaid with an STD spectrum obtained from the GD1a-S-Phe/GB1 complex (bottom). Well-resolved peaks within the spectra are labeled according to the GD1a-S-Phe structure presented in Figure 1. (C) Color-coded model of the oligosaccharide component of GD1a based on levels of STD attenuation. Atoms shaded in red correspond to the most strongly attenuated resonances of the glycan (80−100%). Blue coloring corresponds to those that were weakly saturated (0−40%) and yellow for those with relative values between 40% and 80%. Atoms are colored only if accurate integration measurements could be made for their corresponding peaks in the STD spectra. The percent saturation is normalized with respect to the most strongly saturated resonance in the glycan, which was assigned a value of 100%. The molecular model for the oligosaccharide component of GD1a is based on a Monte Carlo energy minimization calculation.

cases, resonances which exhibit a strong STD response correspond with those that are in closest proximity to the immunoglobulin upon binding.

GB1 Interacts Closely with Sites on Multiple Residues of GD1a-S-Phe. Strong STD signals are observed for several resonances of GD1a-S-Phe, and these are located primarily in the two NeuAc residues (Figure 4). The most prominent peak in the STD spectra arises from the *N*-acetyl methyl resonances of the two NeuAc residues (Figure 4B). Interestingly, the equatorial and axial H3 protons of the same two residues are among the most weakly enhanced in the molecule. The *N*-acetyl methyl protons of GalNAc are not significantly enhanced (Figure 4B). Among the well-resolved peaks in the H-ring and anomeric region of the STD spectra,

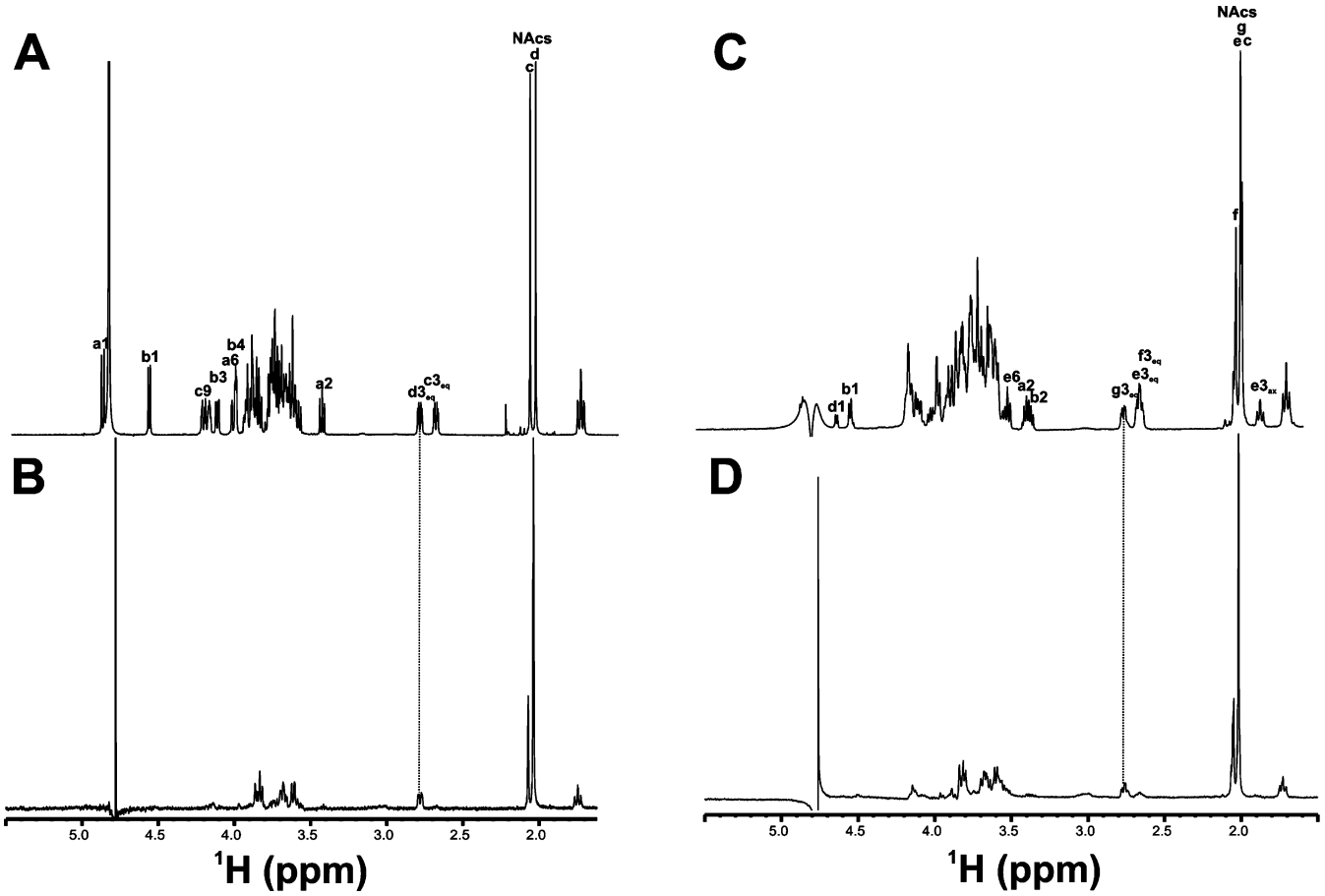

FIGURE 5: FS1 interacts with the terminal NeuAc residue of both GD3-S-Phe and GT1a-S-Phe. Most resonances in 1D ^{1}H spectra of (A) GD3-S-Phe and (C) GT1a-S-Phe are noticeably absent from the corresponding STD spectra of (B) GD3-S-Phe/FS1 and (D) GT1a-S-Phe/FS1 complexes, with the exception of those from the terminal NeuAc residue of the disialosyl moiety. Resonances are labeled on the basis of the ganglioligosaccharide structures presented in Figure 1.

most of the strong STD signals are from protons in the exocyclic side chain of the NeuAc residues (Figure 4A), whereas the majority of the protons from the four neutral sugars forming the backbone of the molecule are generally the more weakly enhanced. To help to rationalize the STD data, an energy-minimized structure representing the glycan component of GD1a was constructed and color-coded on the basis of the relative levels of saturation (Figure 4C). In the model, the oligosaccharide residues are oriented such that the branched NeuAc residues extend, in a perpendicular orientation, from the backbone plane formed by the neutral residues. The portions appearing in red represent the regions that bind most closely with GB1, and these are found mainly within the NeuAc residues.

FS1 Binds to the Terminal NeuAc Residue of GD3-S-Phe and GT1a-S-Phe. The interaction of FS1 with its corresponding gangliooligosaccharides gave rise to STD spectra that were consistent with a tightly confined interaction site. FS1 binding to both GD3-S-Phe and GT1a-S-Phe is limited almost exclusively to the terminal sialic acid of the disialosyl moiety in these molecules. The STD spectra for both complexes are almost identical, indicating that FS1 recognizes the same site in these two ganglioside derivatives (Figure 5B,D). Among the protons that give rise to well-resolved signals in GD3-S-Phe and GT1a-S-Phe, only $H3_{eq}$ and the *N*-acetyl methyl group of the terminal NeuAc are present in the STD spectra, whereas prominent peaks belonging to protons from the other residues are clearly absent. There is some saturation response from the *N*-acetyl methyl resonance belonging to the penultimate NeuAc residue of the disialosyl moiety (Figure 5B,D); however, the relative attenuation is significantly diminished in comparison with that observed for this methyl group in the terminal residue (Figure 3C). There is a complete absence of saturation transfer to any of the remaining resonances of the subterminal NeuAc of the disialosyl moiety.

Further inspection of the STD spectra for the binding of GD3-S-Phe and GT1a-S-Phe to FS1 demonstrates that the close interaction between the immunoglobulin and these two ganglioside derivatives is limited to the *N*-acetylmannosaminyl portion of the terminal NeuAc; there is no close contact with protons found in the exocyclic side chain of this residue (Figure 6). This interaction profile is highlighted when STD spectra for GD3-S-Phe/FS1 are overlaid with selective TOCSY spectra of GD3-S-Phe, where only resonances from the terminal NeuAc residue are excited (Figure 6B,C). The peaks arising from protons in the *N*-acetylmannosaminyl ring (i.e., H3, H4, H5, and H6) are present in the STD spectrum, while, remarkably, there is no saturation transfer to any of the protons of the exocyclic side chain (i.e., H7, H8, and H9) (Figure 6D). Inspection of the STD-TOCSY spectrum (Figure 6E) acquired for the GD3-S-Phe/FS1 pair reveals that cross-peaks are confined to protons in the *N*-acetylmannosaminyl ring of the terminal NeuAc. The STD-TOCSY results confirm that FS1 interaction is limited to this segment

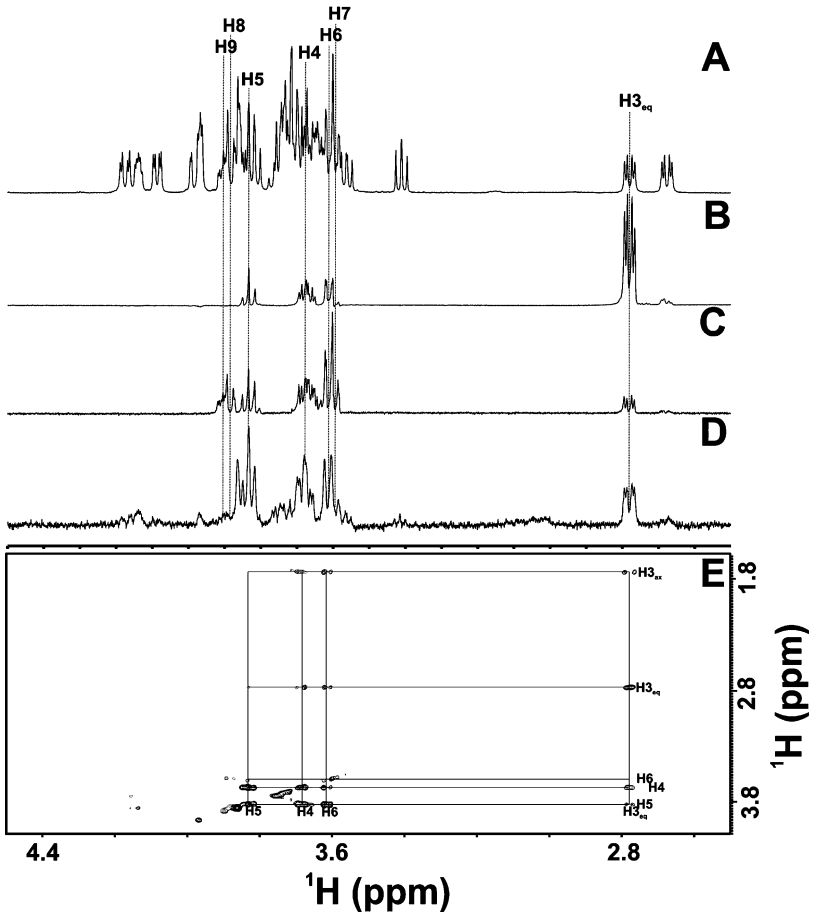

FIGURE 6: FS1 interacts with the *N*-acetylmannosaminyl portion of the terminal NeuAc residue of GD3-S-Phe. (A) Protons from the terminal NeuAc are labeled in a 1D ^{1}H spectrum of GD3-S-Phe. (B) Selective excitation of the $H3_{eq}$ resonance of the terminal NeuAc in a 1D-TOSCY spectrum results in the transfer of magnetization to the other proton resonances within the *N*-acetylmannosaminyl ring (i.e., $H3_{ax}$, H4, H5, and H6). (C) Further selective excitation of H6 in a 1D-TOCSY-TOCSY spectrum results in signal growth for the remaining proton resonances found in the exocylic side chain (i.e., H7, H8, and H9). (D) The STD spectrum of the GD3-S-Phe/FS1 complex clearly shows a strong signal from the protons in the *N*-acetylmannosaminyl ring and not the exocyclic side chain. A similar pattern was observed for the GT1a-S-Phe/FS1 complex. (E) Cross-peaks in an STD-TOCSY spectrum arise from the $H3_{ax}$-$H3_{eq}$-H4-H5-H6 spin system, demonstrating that interaction is confined to the *N*-acetylmannosaminyl ring.

of GD3-S-Phe. A similar pattern is observed in STD spectra of the GT1a-S-Phe/FS1 complex.

DISCUSSION

We have studied the binding characteristics of four mAbs, which were raised against LOS from the GBS- and FS-associated *C. jejuni* strains, CF90-26 and CF93-6, respectively. SPR was used to demonstrate that these immunoglobulins are cross-reactive with the carbohydrate portion of specific gangliosides and provided measures of their binding kinetics. STD NMR was used to elucidate the molecular basis for the interaction of two mAbs (FS1 and GB1) with their targeted oligosaccharides.

SPR Analysis of mAb/Gangliooligosaccharide Interaction. SPR is a technique well suited to establish whether anti-carbohydrate antibodies possess unusual binding affinities or kinetics for gangliosides. This is because SPR enables the determination of equilibrium and kinetic values governing antibody/antigen interaction. We have demonstrated that chemoenzymatically synthesized gangliooligosaccharides can be utilized for this purpose, by providing the first measurements of binding constants for cross-reactive antibodies. The mAbs GB1, GB2, and FS3 showed strong binding specificity for their associated gangliooligosaccharide derivatives. The observed dissociation equilibrium constants (K_D) were on the order of 10−20 μM (Figure 2). These values correspond to a relatively weak binding affinity, typical of anti-carbohydrate mAbs (*38*). With one antibody, FS1, we did not observe quantifiable levels of interaction with any thiophenyl derivative, although we know, from ELISA and STD NMR experiments, that this antibody does specifically recognize the glycan component of GT1a and GD3. The monovalent binding affinity of FS1 for these two oligosaccharides appears to be too weak for characterization by SPR.

STD NMR Studies of mAb/Gangliooligosaccharide Interaction. When each of the four antibodies was incubated in the presence of its targeted oligosaccharide, there were observable STD signals (Figure 3). However, this technique could not provide an epitope map for the interaction of GB2/GM1a-S-Phe or FS3/GT1a-S-Phe because the ligand protons of the oligosaccharides experienced uniform levels of saturation. It is likely that this can be attributed to spin diffusion. In other words, following saturation transfer to the oligosaccharide protons in close proximity to the protein, there was a relay of the saturation effect to the other ligand protons before dissociation. Bax and colleagues (*39*) have calculated that, for the interaction of an antigen with an antibody (MW $\approx$ 150000), the effects of spin diffusion may become

observable if k_{off} is less than 200 s^{-1}. Therefore, in antibody recognition studies by STD NMR, a slow k_{off} is a critical limiting factor. For the mAb/oligosaccharide complexes where dissociation rates could be estimated from SPR analysis, the GB1/GD1a-S-Phe pair had the most rapid k_{off} and was the only system among the three where a differential buildup in saturation transfer occurred (Figure 3B). It is possible that the glycosidic bond linking two monosaccharides could, in principle, isolate an intraresidual spin network and thereby limit the effect of spin diffusion in STD studies with oligosaccharide ligands (*27*). However, interresidual distances separating protons on adjacent residues of an oligosaccharide can be very small. For instance, in our energy-minimized model of the glycan component of GD1a (Figure 4C), the distance between protons across the glycosidic bonds, including those involving sialic acid, was as short as 2.0−2.5 Å. Our results suggest that intramolecular spin diffusion can readily occur in studies with oligosaccharides, and this can prevent effective epitope mapping by STD NMR.

Epitope Map for the Interaction of GB1 with GD1a-S-Phe. The STD NMR profile for the binding of GB1 with GD1a-S-Phe is consistent with a broad distribution of relative STD signals among the oligosaccharide protons (Figure 4). GB1 interacts closely with several regions of GD1a-S-Phe. Most of the strongly saturated protons are located in the two NeuAc residues, which are spatially separated from each other (Figure 4). There was also strong saturation of the H2 resonance belonging to the subterminal βGal residue. The recognition of GD1a-S-Phe by GB1 is consistent with our understanding of glycan binding by anti-carbohydrate antibodies. On the basis of available crystallographic structures (*40*−*42*), interaction sites are not defined, topologically, as deep clefts or binding pockets. Protein−glycan contacts tend to occur in shallow cavities, and the binding region can accommodate interaction with parts of several residues of an oligosaccharide (*43*).

Epitope Map for the Interaction of FS1 with Disialosyl-Containing Oligosaccharides. FS1 binding with either GD3-S-Phe or GT1a-S-Phe is confined narrowly to the *N*-acetylmannosaminyl ring portion of the terminal sialic acid residue (Figure 6). As opposed to the interaction profile observed with GB1/GD1a-S-Phe, the saturation transfer resulting from FS1 binding to its targeted oligosaccharides is best described as an *all-or-none* process, because only a small number of ligand protons exhibited an STD response. It was surprising to find in FS1 an antibody with such a confined antigen recognition site. Nevertheless, the interaction profile provides a mechanistic understanding for how a unique LOS-bound ganglioside mimic can give rise to an antibody with binding promiscuity for [αNeuAc-(*2*−*8*)-αNeuAc]-bound epitopes.

Serum anti-GQ1b IgG antibodies from FS patients invariably cross-react with GT1a and sometimes with GD3, GD2, GD1b, and GT1b (*44*). Antibodies with binding characteristics similar to FS1 are perhaps responsible for the cross-reactivity seen in the sera of FS patients. The limited structural data regarding carbohydrate/antibody interaction, however, make it difficult to speculate as to how unique the recognition pattern for FS1 is. Such conclusions await further crystallographic and NMR-based structural studies focused on other FS-associated antibodies and, more generally, those that are involved in carbohydrate recognition.

ACKNOWLEDGMENT

We thank Anna Cunningham, Marie-France Karwaski, and Denis Brochu for technical assistance and Drs. Warren Wakarchuk, Wojciech Jachymek, and Roger MacKenzie for helpful discussions.

SUPPORTING INFORMATION AVAILABLE

The ^{1}H and ^{13}C chemical shift assignments for GD3-S-Phe, GM1a-S-Phe, GD1a-S-Phe, and GT1a-S-Phe (Tables S1 and S2). This material is available free of charge via the Internet at http://pubs.acs.org.

REFERENCES

1. Ang, C. W., Jacobs, B. C., and Laman, J. D. (2004) The Guillain-Barré syndrome: A true case of molecular mimicry, *Trends Immunol. 25*, 61−66.
2. Willison, H. J. (2005) The immunobiology of Guillain-Barré syndromes, *J. Peripher. Nerv. Syst. 10*, 94−112.
3. Yuki, N. (2005) Carbohydrate mimicry: A new paradigm of autoimmune diseases, *Curr. Opin. Immunol. 17*, 577−582.
4. Jacobs, B. C., Rothbarth, P. H., van der Meche, F. G., Herbrink, P., Schmitz, P. I., de Klerk, M. A., and van Doorn, P. A. (1998) The spectrum of antecedent infections in Guillain-Barré syndrome: A case-control study, *Neurology 51*, 1110−1115.
5. Koga, M., Gilbert, M., Li, J., Koike, S., Takahashi, M., Furukawa, K., Hirata, K., and Yuki, N. (2005) Antecedent infections in Fisher syndrome: A common pathogenesis of molecular mimicry, *Neurology 64*, 1605−1611.
6. Aspinall, G. O., McDonald, A. G., Pang, H., Kurjanczyk, L. A., and Penner, J. L. (1994) Lipopolysaccharides of *Campylobacter jejuni* serotype O:19: Structures of core oligosaccharide regions from the serostrain and two bacterial isolates from patients with the Guillain-Barré syndrome, *Biochemistry 33*, 241−249.
7. Koga, M., Gilbert, M., Takahashi, M., Li, J., Koike, S., Hirata, K., and Yuki, N. (2006) Comprehensive analysis of bacterial risk factors for the development of Guillain-Barré syndrome after *Campylobacter jejuni* enteritis, *J. Infect. Dis. 193*, 547−555.
8. Shin, J. E., Ackloo, S., Mainkar, A. S., Monteiro, M. A., Pang, H., Penner, J. L., and Aspinall, G. O. (1997) Lipo-oligosaccharides of *Campylobacter jejuni* serotype O:10: Structures of core oligosaccharide regions from a bacterial isolate from a patient with the Miller-Fisher syndrome and from the serotype reference strain, *Carbohydr. Res. 305*, 223−232.
9. Yuki, N., Taki, T., Inagaki, F., Kasama, T., Takahashi, M., Saito, K., Handa, S., and Miyatake, T. (1993) A bacterium lipopolysaccharide that elicits Guillain-Barré syndrome has a GM1 ganglioside-like structure, *J. Exp. Med. 178*, 1771−1775.
10. Goodyear, C. S., O'Hanlon, G. M., Plomp, J. J., Wagner, E. R., Morrison, I., Veitch, J., Cochrane, L., Bullens, R. W., Molenaar, P. C., Conner, J., and Willison, H. J. (1999) Monoclonal antibodies raised against Guillain-Barré syndrome-associated Campylobacter jejuni lipopolysaccharides react with neuronal gangliosides and paralyze muscle-nerve preparations, *J. Clin. Invest. 104*, 697−708.
11. Caporale, C. M., Capasso, M., Luciani, M., Prencipe, V., Creati, B., Gandolfi, P., De Angelis, M. V., Di, M. A., Caporale, V., and Uncini, A. (2006) Experimental axonopathy induced by immunization with *Campylobacter jejuni* lipopolysaccharide from a patient with Guillain-Barré syndrome, *J. Neuroimmunol. 174*, 12−20.
12. Yuki, N., Susuki, K., Koga, M., Nishimoto, Y., Odaka, M., Hirata, K., Taguchi, K., Miyatake, T., Furukawa, K., Kobata, T., and Yamada, M. (2004) Carbohydrate mimicry between human ganglioside GM1 and *Campylobacter jejuni* lipooligosaccharide causes Guillain-Barré syndrome, *Proc. Natl. Acad. Sci. U.S.A. 101*, 11404−11409.
13. Godschalk, P. C., Heikema, A. P., Gilbert, M., Komagamine, T., Ang, C. W., Glerum, J., Brochu, D., Li, J., Yuki, N., Jacobs, B. C., van Belkum, A., and Endtz, H. P. (2004) The crucial role of *Campylobacter jejuni* genes in anti-ganglioside antibody induction in Guillain-Barré syndrome, *J. Clin. Invest. 114*, 1659−1665.
14. Parker, C. T., Horn, S. T., Gilbert, M., Miller, W. G., Woodward, D. L., and Mandrell, R. E. (2005) Comparison of *Campylobacter*

jejuni lipooligosaccharide biosynthesis loci from a variety of sources, *J. Clin. Microbiol. 43*, 2771−2781.
15. Willison, H. J., and Yuki, N. (2002) Peripheral neuropathies and anti-glycolipid antibodies, *Brain 125*, 2591−2625.
16. Gilbert, M., Brisson, J. R., Karwaski, M. F., Michniewicz, J., Cunningham, A. M., Wu, Y., Young, N. M., and Wakarchuk, W. W. (2000) Biosynthesis of ganglioside mimics in *Campylobacter jejuni* OH4384: Identification of the glycosyltransferase genes, enzymatic synthesis of model compounds, and characterization of nanomole amounts by 600-mHz ^{1}H and ^{13}C NMR analysis, *J. Biol. Chem. 275*, 3896−3906.
17. Gilbert, M., Karwaski, M. F., Bernatchez, S., Young, N. M., Taboada, E., Michniewicz, J., Cunningham, A. M., and Wakarchuk, W. W. (2002) The genetic bases for the variation in the lipo-oligosaccharide of the mucosal pathogen, *Campylobacter jejuni*: Biosynthesis of sialylated ganglioside mimics in the core oligosaccharide, *J. Biol. Chem. 277*, 327−337.
18. Blixt, O., Vasiliu, D., Allin, K., Jacobsen, N., Warnock, D., Razi, N., Paulson, J. C., Bernatchez, S., Gilbert, M., and Wakarchuk, W. (2005) Chemoenzymatic synthesis of 2-azidoethyl-ganglio-oligosaccharides GD3, GT3, GM2, GD2, GT2, GM1, and GD1a, *Carbohydr. Res. 340*, 1963−1972.
19. Brisson, J. R., Sue, S. C., Wu, W. G., McManus, G., Nghia, P. T., and Uhrin, D. (2002) in *NMR Spectroscopy of Glycoconjugates* (Jimenez-Barbero, J., and Peters, T., Eds.) pp 59−93, Wiley-VCH, Weinhem, Germany.
20. Peters, T., Meyer, B., Stuike-Prill, R., Somorjai, R., and Brisson, J. R. (1993) A Monte Carlo method for conformational analysis of saccharides, *Carbohydr. Res. 238*, 49−73.
21. Sabesan, S., Duus, J. O., Fukunaga, T., Bock, K., and Ludvigsen, S. (1991) NMR and conformational analysis of ganglioside GD1a, *J. Am. Chem. Soc. 113*, 3236−3246.
22. Mayer, M., and Meyer, B. (2001) Group epitope mapping by saturation transfer difference NMR to identify segments of a ligand in direct contact with a protein receptor, *J. Am. Chem. Soc. 123*, 6108−6117.
23. McCoy, M. A., Senior, M. M., and Wyss, D. F. (2005) Screening of protein kinases by ATP-STD NMR spectroscopy, *J. Am. Chem. Soc. 127*, 7978−7979.
24. Bhunia, A., Jayalakshmi, V., Benie, A. J., Schuster, O., Kelm, S., Rama, K. N., and Peters, T. (2004) Saturation transfer difference NMR and computational modeling of a sialoadhesin-sialyl lactose complex, *Carbohydr. Res. 339*, 259−267.
25. Johnson, M. A., and Pinto, B. M. (2002) Saturation transfer difference 1D-TOCSY experiments to map the topography of oligosaccharides recognized by a monoclonal antibody directed against the cell-wall polysaccharide of group A *Streptococcus*, *J. Am. Chem. Soc. 124*, 15368−15374.
26. Kooistra, O., Herfurth, L., Luneberg, E., Frosch, M., Peters, T., and Zahringer, U. (2002) Epitope mapping of the O-chain polysaccharide of *Legionella pneumophila* serogroup 1 lipopolysaccharide by saturation-transfer-difference NMR spectroscopy, *Eur. J. Biochem. 269*, 573−582.
27. Maaheimo, H., Kosma, P., Brade, L., Brade, H., and Peters, T. (2000) Mapping the binding of synthetic disaccharides representing epitopes of chlamydial lipopolysaccharide to antibodies with NMR, *Biochemistry 39*, 12778−12788.
28. Rinnbauer, M., Ernst, B., Wagner, B., Magnani, J., Benie, A. J., and Peters, T. (2003) Epitope mapping of sialyl Lewis (x) bound to E-selectin using saturation transfer difference NMR experiments, *Glycobiology 13*, 435−443.
29. Sandström, C., Berteau, O., Gemma, E., Oscarson, S., Kenne, L., and Gronenborn, A. M. (2004) Atomic mapping of the interactions between the antiviral agent cyanovirin-N and oligomannosides by saturation-transfer difference NMR, *Biochemistry 43*, 13926−13931.
30. Herfurth, L., Ernst, B., Wagner, B., Ricklin, D., Strasser, D. S., Magnani, J. L., Benie, A. J., and Peters, T. (2005) Comparative epitope mapping with saturation transfer difference NMR of sialyl Lewis (a) compounds and derivatives bound to a monoclonal antibody, *J. Med. Chem. 48*, 6879−6886.
31. Haselhorst, T., Wilson, J. C., Liakatos, A., Kiefel, M. J., Dyason, J. C., and von Itzstein, M. (2004) NMR spectroscopic and molecular modeling investigations of the trans-sialidase from *Trypanosoma cruzi*, *Glycobiology 14*, 895−907.
32. Haselhorst, T., Munster-Kuhnel, A. K., Stolz, A., Oschlies, M., Tiralongo, J., Kitajima, K., Gerardy-Schahn, R., and von Itzstein, M. (2005) Probing a CMP-Kdn synthetase by ^{1}H, ^{31}P, and STD NMR spectroscopy, *Biochem. Biophys. Res. Commun. 327*, 565−570.
33. Haselhorst, T., Oschlies, M., bu-Izneid, T., Kiefel, M. J., Tiralongo, J., Munster-Kuhnel, A. K., Gerardy-Schahn, R., and von Itzstein, M. (2006) A ^{1}H STD NMR spectroscopic investigation of sialylnucleoside mimetics as probes of CMP-Kdn synthetase, *Glycoconjugate J. 23*, 371−375.
34. Clement, M. J., Fortune, A., Phalipon, A., Marcel-Peyre, V., Simenel, C., Imberty, A., Delepierre, M., and Mulard, L. A. (2006) Toward a better understanding of the basis of the molecular mimicry of polysaccharide antigens by peptides: The example of *Shigella flexneri* 5a, *J. Biol. Chem. 281*, 2317−2332.
35. Johnson, M. A., and Pinto, B. M. (2004) Saturation-transfer difference NMR studies for the epitope mapping of a carbohydrate-mimetic peptide recognized by an anti-carbohydrate antibody, *Bioorg. Med. Chem. 12*, 295−300.
36. Moller, H., Serttas, N., Paulsen, H., Burchell, J. M., and Taylor-Papadimitriou, J. (2002) NMR-based determination of the binding epitope and conformational analysis of MUC-1 glycopeptides and peptides bound to the breast cancer-selective monoclonal antibody SM3, *Eur. J. Biochem. 269*, 1444−1455.
37. Jayalakshmi, V., and Krishna, N. R. (2005) Determination of the conformation of trimethoprim in the binding pocket of bovine dihydrofolate reductase from a STD-NMR intensity-restrained CORCEMA-ST optimization, *J. Am. Chem. Soc. 127*, 14080−14084.
38. MacKenzie, C. R., Hirama, T., Deng, S. J., Bundle, D. R., Narang, S. A., and Young, N. M. (1996) Analysis by surface plasmon resonance of the influence of valence on the ligand binding affinity and kinetics of an anti-carbohydrate antibody, *J. Biol. Chem. 271*, 1527−1533.
39. Glaudemans, C. P., Lerner, L., Daves, G. D., Jr., Kovac, P., Venable, R., and Bax, A. (1990) Significant conformational changes in an antigenic carbohydrate epitope upon binding to a monoclonal antibody, *Biochemistry 29*, 10906−10911.
40. Cygler, M., Rose, D. R., and Bundle, D. R. (1991) Recognition of a cell-surface oligosaccharide of pathogenic *Salmonella* by an antibody Fab fragment, *Science 253*, 442−445.
41. Cygler, M., Wu, S., Zdanov, A., Bundle, D. R., and Rose, D. R. (1993) Recognition of a carbohydrate antigenic determinant of *Salmonella* by an antibody, *Biochem. Soc. Trans. 21*, 437−441.
42. Vyas, M. N., Vyas, N. K., Meikle, P. J., Sinnott, B., Pinto, B. M., Bundle, D. R., and Quiocho, F. A. (1993) Preliminary crystallographic analysis of a Fab specific for the O-antigen of *Shigella flexneri* cell surface lipopolysaccharide with and without bound saccharides, *J. Mol. Biol. 231*, 133−136.
43. Bundle, D. R. (1997) Antibody-oligosaccharide interactions determined by crystallography, in *Glycosciences: Status and Perspectives* (Gabius, H.-J., and Gabius, S., Eds.) pp 311−331, Chapman and Hall, Weinheim, Germany.
44. Susuki, K., Yuki, N., and Hirata, K. (2001) Fine specificity of anti-GQ1b IgG and clinical features, *J. Neurol. Sci. 185*, 5−9.

BI062001V